Bifurcation Control of Power Electronic DC-DC Converters

Somnath Maity, Damian Giaouris, Soumitro Banerjee, Tapas K. Bhattacharya, Bashar Zahawi, and Volker Pickert

***Abstract*— Power electronic dc-dc converters widely used in industry are known to exhibit undesirable subharmonic and chaotic behaviour beyond certain parameter ranges. In this paper we propose methods of controlling the bifurcation to extend the range of desirable period-1 operation, by taking advantage of the switching nature of such circuits. At the switching events, the evolution of perturbation is given by the so-called "saltation matrix" and hence it is possible to influence the Floquet exponents by manipulating this matrix. In physical terms this implies controlling the triangular wave used in the pulse-width modulator, or using a control logic that uses voltage as well as current feedback. We demonstrate the resulting control of the bifurcation both by simulation and by experiment.**

***Index Terms*— Bifurcation control, dc-dc converters, saltation matrix, monodromy matrix.**

I. Introduction

Power electronic circuits are variable structure systems and give rise to a great variety of nonlinear behaviors, e.g., period doubling route to chaos [1], border collision bifurcation [1], grazing phenomena [2] and quasi-periodicity [3], [4]. Because of these apparently unpredictable and often undesirable oscillatory behaviors, their control has become a topic of interest in the recent past [5]. The ability to avoid chaos and other nonlinear behaviors is almost a basic feature of all existing practical control strategies. Various control techniques have been proposed by means of feedback control actions aimed at changing the system dynamics over the entire region of interest [6], [7], [8]. Other non-feedback control methods [9] have also been proposed, which are highly suitable for suppressing chaos and bifurcation in periodically driven systems [10], [9].

In this paper, we consider a new non-feedback parametric perturbation for controlling bifurcation in a PWM voltage-mode controlled buck converter based on suitably changing the slope of the switching manifold. In general, parametric perturbation can make a system chaotic, but applying it at appropriate frequencies and magnitudes can induce the system to stay in periodic regimes [11]. We also show the effect of perturbed signal on system's stability using Filippov solution [12].

II. Mathematical Model of the Converter

We consider a voltage-mode controlled buck converter as shown in Fig.1. It consists of a controlled switch S (MOSFET), an uncontrolled switch D (diode), an inductor L, a capacitor C, and a load resistance R. The switching of the MOSFET is controlled by feedback logic known as pulse width modulation of type-2 (PWM-2). This is achieved by obtaining a control voltage $v_{\rm con}$, as a linear combination of the output capacitor voltage v, and a reference signal $V_{\rm ref}$ in the form

$$v_{\rm con} = \alpha(V_{\rm ref} - v/k_1), \tag{1}$$

where α is the gain of the error amplifier and k_1 is the factor of reduction of the output voltage v. An externally generated saw-tooth voltage $V_{\rm ramp} = V_l + (V_u - V_l)F(t/T)$, of time period T and upper and lower threshold voltages V_u and V_l respectively, is used to determine the switching instants. Here $F(x)$ denotes the fractional part of x : $\{F(x) = x \bmod 1\}$. In PWM-2, the controlled voltage $v_{\rm con}$ is then compared with the periodic saw-tooth wave $V_{\rm ramp}$, to generate the switching signal $q(t) \in [1, 0]$ described by

$$\begin{aligned} &\text{If} \quad V_{\rm ramp} > v_{\rm con}; \quad p(t) = 1, \\ &\text{If} \quad V_{\rm ramp} < v_{\rm con}; \quad p(t) = 0. \end{aligned}$$

The inductor current increases while switch S is *on* i.e. $p(t) = 1$ and falls while switch S is *off* i.e. $p(t) = 0$. The buck converter can be regarded as a second-order nonautonomous continuous dynamical system, which can be described by a state equation of the form

$$\dot{\mathbf{x}} = \mathbf{f}(\mathbf{x}, t) \tag{2}$$

where $\mathbf{x} = [i \quad v]^T$ is the state vector and $f(\mathbf{x}, t)$ is the vector field. Under normal operation, the system is nonautonomous because the vector field $\mathbf{f}(\mathbf{x}, t)$ is a function of time. Moreover, the system is periodic with period T since $\mathbf{f}(\mathbf{x}, t) = \mathbf{f}(\mathbf{x}, t+T)$ for any t. When the system assumes a specific circuit topology, the corresponding vector field is linear and continuous. However, the vector field of the system becomes discontinuous at the switching instants where the circuit topology is changed[1].

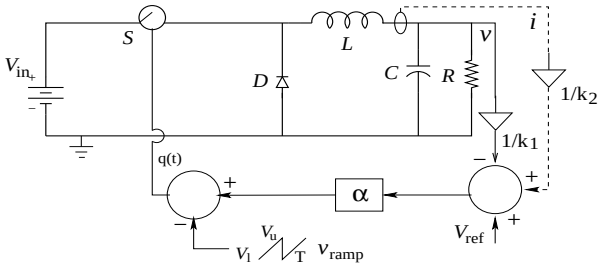

Fig. 1. Voltage-mode controlled buck converter.

Somnath Maity,Soumitro Banerjee and Tapas K. Bhattacharya are with the Indian Institute of Technology, Kharagpur-721302, India. E−mail addresses: smaity, soumitro, tapas@ee.iitkgp.ernet.in

Damian Giaouris, Bashar Zahawi, and Volker Pickert School of Electrical, Electronics and Computer Engineering, University of Newcastle upon tyne, UK.E−mail address: Damian Giaouris@newcastle.ac.uk

[1]At switching points, the state vector changes its orientation; the vector field, being the time derivative of the state vector, is discontinuous.

Thus the overall vector field is discontinuous and the system is a *piecewise-smooth dynamical system*. Specifically, the vector field $\mathbf{f}(\mathbf{x},t)$ can be defined as

$$\frac{dx_1}{dt} = \begin{cases} V_{\rm in}/L - x_2/L; & \alpha(V_{\rm ref}-x_2/k_1) > V_{\rm ramp}, \\ -x_2/L; & \alpha(V_{\rm ref}-x_2/k_1) < V_{\rm ramp}. \end{cases} \quad (3)$$

$$\frac{dx_2}{dt} = x_1/C - x_2/RC. \quad (4)$$

The switching event occurs whenever the vector field of each circuit topology reaches the border function $h(\mathbf{x},t)$ defined by

$$h(\mathbf{x},t) = \alpha(V_{\rm ref}-x_2/k_1) - \frac{(V_u-V_l)t}{T} - V_l = 0; \quad (5)$$

Subsequently the evolution of $\mathbf{x}$ is governed by (3) and (4). Therefore, the two dimensional state-space can be divided into three parts:

$$\mathbf{x}_- \cup \Sigma \cup \mathbf{x}_+ = \Re^2 \quad (6)$$

where

$$\begin{aligned} V_-: \mathbf{x}_- &= \{\mathbf{x} \in \Re^2 : h(\mathbf{x},t) < 0\}, \\ V_+: \mathbf{x}_+ &= \{\mathbf{x} \in \Re^2 : h(\mathbf{x},t) > 0\}, \\ \Sigma &= \{\mathbf{x} \in \Re^2 : h(\mathbf{x},t) = 0\}. \end{aligned}$$

Hence, (6) can be written as

$$\dot{\mathbf{x}} = \mathbf{f}(\mathbf{x},t) = \begin{cases} \mathbf{f}_-(\mathbf{x},t); & \mathbf{x} \in V_- \\ \overline{co}\{\mathbf{f}_-(\mathbf{x},t), \mathbf{f}_+(\mathbf{x},t)\}; & \mathbf{x} \in \Sigma \\ \mathbf{f}_+(\mathbf{x},t); & \mathbf{x} \in V_+ \end{cases} \quad (7)$$

In the sense of Filippov's convex method, (3) and (4) can be written as an upper semi-continuous $\mathbf{f}(\mathbf{x},t)$ and (7) has a solution if the vector fields enter the hyper-surface Σ instantaneously. Since there is only one discontinuity at the switching hyper-surface as shown in Fig.2 the convex hall is defined as

$$\overline{co}\{\mathbf{f}_-(\mathbf{x},t), \mathbf{f}_+(\mathbf{x},t)\} = \begin{bmatrix} \overline{co}\{(V_{\rm in}-x_2)/L, -x_2/L\} \\ x_1/C - x_2/RC \end{bmatrix}$$

$$= \begin{bmatrix} \{(1-q)(V_{\rm in}/L - x_2/L) - qx_2/L\} \\ x_1/C - x_2/RC \end{bmatrix}, \ \forall q \in [0,1]$$

The normal to switching hyper-surface $\mathbf{n}$ is

$$\mathbf{n} = \nabla h(\mathbf{x},t) = \begin{bmatrix} \frac{\partial h(\mathbf{x},t)}{\partial x_1} & \frac{\partial h(\mathbf{x},t)}{\partial x_2} \end{bmatrix}^T = [0 \quad -1/k_1]^T \quad (8)$$

Therefore, the projections of $\mathbf{f}_-$ and $\mathbf{f}_+$ on Σ are given by

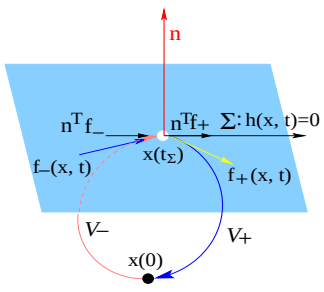

Fig. 2. Switching surface.

$$\mathbf{n}^{\mathbf{T}}\mathbf{f}_- = -x_1/C + x_2/RC, \ \ \mathbf{n}^{\mathbf{T}}\mathbf{f}_+ = -x_1/C + x_2/RC$$

Since, $\mathbf{n}^{\mathbf{T}}\mathbf{f}_-.\mathbf{n}^{\mathbf{T}}\mathbf{f}_+ > 0$, the vector fields transversely intersect the switching manifold Σ.

Assuming a periodic orbit starts at $t = t_0$ in subsystem V_-, intersect the switching surface at $t = t_\Sigma$ (or $t = dT$), goes over to subsystem V_+ and return to initial condition at $t = t_0 + T$. Before the intersection with the switching surface Σ, the system is smooth and therefore the fundamental matrix before and after the intersection can be defined as [12]

$$\begin{aligned} \mathbf{W}(t_1,t_0,\mathbf{x}_0) &= e^{A_s(t_1-t_0)}; \ \forall\, t_1 \in (t_0,t_\Sigma), \\ \mathbf{W}(t_2,t_\Sigma,\mathbf{x}_\Sigma) &= e^{A_s(t_2-t_\Sigma)}; \ \forall\, t_2 \in (t_\Sigma,T). \end{aligned}$$

where

$$A_s = \begin{bmatrix} 0 & -1/L \\ 1/C & -1/RC \end{bmatrix},$$

The state transition matrix $\mathbf{W}(t_0+T,t_0,\mathbf{x}(t_0))$ calculated over a complete cycle (the *Monodromy Matrix*) is defined as

$$\mathbf{W}(T+t_0,t_0,\mathbf{x}(t_0)) = \mathbf{W}(T+t_0,t_\Sigma,\mathbf{x}_\Sigma)\mathbf{S}\mathbf{W}(t_\Sigma,t_0,\mathbf{x}_0) \quad (9)$$

The *saltation matrix* $\mathbf{S}$ defines the solution on the hyper-surface at $t = t_\Sigma$ and is given by

$$\mathbf{S} = \mathbf{I} + \frac{\left[\lim_{t\to t_{\Sigma+}} f_+(\mathbf{x},t) - \lim_{t\to t_{\Sigma-}} \mathbf{f}_-(\mathbf{x},t)\right]\mathbf{n}^{\mathbf{T}}}{\mathbf{n}^{\mathbf{T}} \lim_{t\to t_{\Sigma-}} \mathbf{f}_-(\mathbf{x},t) + \frac{\partial h}{\partial t}(\mathbf{x},t)|_{t_\Sigma}} \quad (10)$$

where $t_{\Sigma-}$ and $t_{\Sigma+}$ denote the time instant just before and after the switching event. The time derivative of the switching hyper-surface is

$$\frac{\partial h(\mathbf{x},t)}{\partial t} = \frac{\partial}{\partial t}\left[V_{\rm ref} - x_2/k_1 - \frac{V_l + (V_u - V_l)t}{\alpha T}\right] = -\frac{V_u - V_l}{\alpha T}$$

Substituting (7) into (10), the saltation matrix $\mathbf{S}$ becomes

$$\mathbf{S} = \begin{bmatrix} 1 & \frac{V_{\rm in}/L}{x_1(t_\Sigma)/C - x_2(t_\Sigma)/RC - (V_u-V_l)/\alpha T} \\ 0 & 1 \end{bmatrix}$$

So, if $\mathbf{S}$ is known it is possible to find out the eigenvalues of monodromy matrix $\mathbf{W}(t_0+T,t_0,\mathbf{x}(t_0))$. For stable period-one fixed point, the absolute magnitude of the eigenvalues must be less than 1.

III. Stability Analysis

Due to the transcendental form of the equation in PWM-2 voltage controlled buck converters [2], it impossible to calculate the exact switching instant within the periodic cycle. The state vector at the switching instant at $t = t_\Sigma$ can be obtained semi-analytically as

$$\mathbf{x}(dT) = \Phi_1(dT)\mathbf{x}(0) + \int_0^{dT} e^{A_s(T-\tau)} B_s d\tau \quad (11)$$

where $B_s = [V_{\rm in}/L \quad 0]^T$ and the duty ratio $d = t_{on}/T = (T - t_\Sigma)/T$. For normal period-1 operation, the value of the state vector at the next clock instant $x(T) = x(0)$ can be easily evaluated as:

$$\mathbf{x}(0) = [\mathbf{I} - e^{A_s T}]^{-1}\left[e^{A_s(T-dT)} A_s^{-1}[\mathbf{I} - e^{A_s T}]B_s\right] \quad (12)$$

which satisfy the hyper-surface

$$V_{\rm ref} - \frac{V_L + (V_u - V_l)d}{\alpha} = [0 \quad 1]e^{A_s dT}\mathbf{x}(0) \quad (13)$$

The solution gives the steady state period-one duty ratio. To analyse the effect of parametric perturbation on the stability of the buck converter (Fig.1), we use the following parameter values: $L = 20mH$, $R = 58\Omega$ $C = 47\mu F$, $\alpha = 10$, V_L=0.4V, V_U=5.8V, $T = 350\mu sec$, V_{ref}=11.3V, and V_{in} is taken as the bifurcation parameter. For $V_{\text{in}} = 30.4$ V [2], numerically we obtain $d = 0.3646$, $\mathbf{x}(0) = [0.1293 \quad 11.0608]^T$, and $\mathbf{x}(dT) = [0.2529 \quad 11.0631]^T$. The saltation matrix and monodromy matrix are calculated as:

$$\mathbf{S} = \begin{bmatrix} 1 & -0.5306 \\ 0 & 1 \end{bmatrix}, \quad \mathbf{W}(\mathbf{T}, \mathbf{0}, \mathbf{x}(\mathbf{0})) = \begin{bmatrix} -0.4294 & -0.5052 \\ 0.5167 & -1.4405 \end{bmatrix}$$

The eigenvalues of the monodromy matrix are $-0.9349 \pm 0.0735j$ implying that at the above parameter values the system is stable. This is in agreement with both numerical (Fig.3a) and experimental observations (Fig.4a).

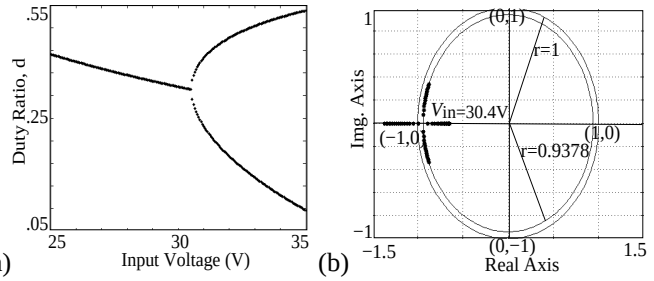

Fig. 3. (a) Bifurcation diagram of duty cycle and (b) eigenvalues loci for $V_{\text{in}} \in (29, 32)$ V for $\delta V = 0$V.

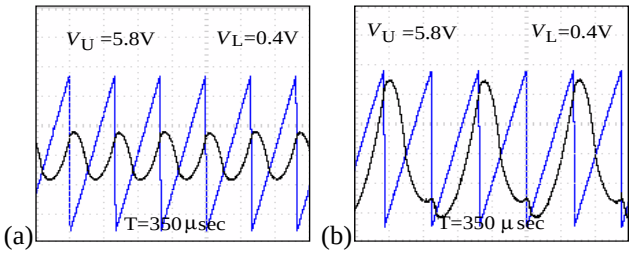

Fig. 4. Experimental results showing (a) normal period-1 operation at $V_{\text{in}} \approx$ 33V, (b) a period 2 operation for $V_{\text{in}} \approx$ 41.6 V.

To confirm the result obtained by Filippov solution methods, we calculated the Floquet multipliers (eigenvalues of the monodromy matrix) for V_{in} ranging from 29 V to 32 V. The locus of the eigenvalues shown in Fig.3b. It shows that eigenvalues first become real at parameter value 30.4 V, then one of the eigenvalues goes through the negative real axis and later it makes the system unstable through a smooth period doubling bifurcation.

IV. Bifurcation Control

It has been shown that the previous analysis gives similar results as the Jacobian of the Poincaré map and is much easier to be used. But more interestingly this method offers a further insight into the converter's operation. It can be seen that the stability depends on the 3 transition matrices and hence it can be claimed that by appropriately changing them we can avoid smooth and nonsmooth bifurcation by keeping the eigenvalues fixed. The monodromy matrix depends heavily on the saltation matrix and hence by influencing that we can avoid fast-scale instabilities. To do that we can either change $\partial h/\partial t$ or we can change the slope of the switching manifold. One way to achieve that is to add a time varying signal to the demanded voltage. This can be a sinusoidal signal $a \sin \omega_s t$ with amplitude a and frequency ω_s. However, depending on the relationship between the switching frequency ω and ω_s, different window lengths of intermittent subharmonics may appear[11]. In the following subsections alternative methods are propose that are easy to implement and guarantee stability over a wide range of the bifurcation variable.

A. Ramp slope change

To overcome these difficulties we choose a different approach to influence the saltation matrix. This is based on the slope of the ramp voltage $m = (V_u - V_l)/T$ as the perturbed parameter and is achieved by changing either the upper tip of ramp voltage V_u, or lower tip of ramp signal V_l, where the strength of the perturbed signal amplitude δV is decided by the ripple magnitude of any state vector. Hence, changing the time derivative of the switching surface to

$$\frac{\partial \mathbf{h}(\mathbf{x}, t)}{\partial t} = \frac{-(V_U - V_L + \delta V)}{\alpha T} \tag{14}$$

To study the effect of increased amplitude perturbation δV, we plot the calculated Floquet multipliers of the monodromy matrix for $V_{\text{in}} \in (29 - 32)V$ and $\delta V_U = 0.4V$ as shown in Fig.5a. Throughout the voltage variation, the absolute value of the eigenvalues $\lambda_{1,2} = 0.9378 < 1$. Based on these results we can propose a new control scheme that will optimally choose the strength of V_u to keep the magnitude of the eigenvalues exactly the same as that for the stable period-1 orbit obtained for a nominal value of V_{U}. This is obtained by solving the the equation: $|eig(\mathbf{W}(T, 0, \mathbf{x}(0))| - 0.9378 = 0$. The results of this algorithm for various values of V_{in} are shown in Fig.**??**b.

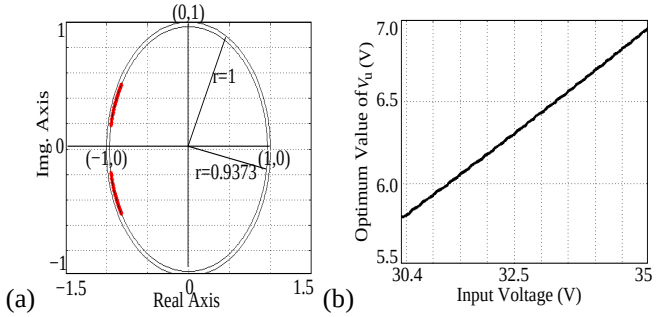

Fig. 5. (a) Eigenvalues loci for $V_{\text{in}} \in (29, 32)$ V for $\delta V = 0.4$V and (b) optimum values of V_u for varying V_{in}.

To further validate these results, experimental tests have been carried out as shown in Fig.6. Results presented in Fig.6b show through the experimentally obtained bifurcation diagram that is possible to push the first period doubling to 42V by adding a small perturbation $\delta V = 0.7V$. To further enhanse the stable area of the system the pertubation is increased to

[2]During experimental results we used 33V, this discrepancy is due to mismatches between the ideal and real values of various parameters

$\delta V = 1.2V$ and it is clear that the system remains stable for the entire operating region. The results are in total agreement with the theoretical prediction as explained earlier.

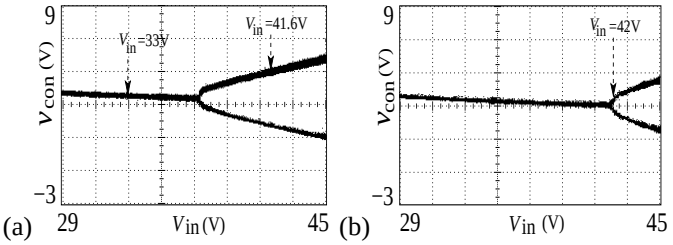

Fig. 6. Experimental bifurcation diagram for (a) $\delta V = 0V$ and (b) $\delta V = 0.7V$

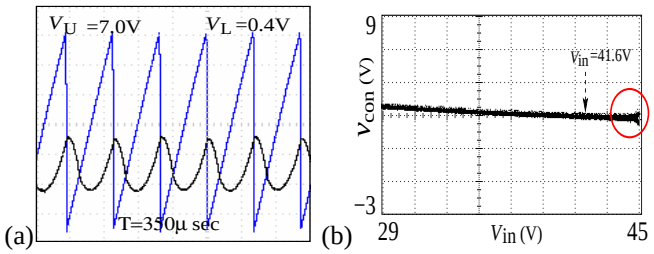

Fig. 7. Experimental results for $\delta V = 1.2V$ (a) period 1 operation and (b) bifurcation diagram

B. Manifold slope change

As the slope of the switching manifold is expressed by its normal vector it is possible to stabilise the system by adding a current component to the feedback signal. This will force the first coordinate of **n** to be nonzero and hence we change the slope of h. In this case the modified switching hyper-surface can be expressed as

$$\mathbf{h}(\mathbf{x},t) = V_{\text{ref}} + x_1/k_2 - x_2/k_1 - V_{\text{ramp}}/\alpha = 0,\ \alpha \neq 0 \quad (15)$$

The normal to switching hyper-surface **n** is

$$\mathbf{n} = \nabla h(\mathbf{x},t) = [1/k_2 \quad -1/k_1]^T \quad (16)$$

Hence in addition to voltage feedback ($k_1 = 1$), the current feedback loop changes the system dynamics. The system becomes stable for a larger parameter range for appropriate feedback gain. To ensure that, it is necessary to calculate the eigenvalues for a wide range of V_{in} and to prove that the period-1 orbit will remain stable. The representative parameter space for $k_2 = 0.1$ is shown in Fig.8 keeping all other parameters same as mentioned before. Through out the voltage range $V_{\text{in}} \in (29-32)$V, the eigenvalues are complex conjugate with absolute magnitude $|\lambda_{1,2}| = 0.9628 < 1$.

As it can be seen by the addition of k_2 the bifurcation pattern did not change but is delayed. This can be deduced by the fact that the eigenvalues follow a similar path as before, (Figs. 8 and 5a). This is very important because it underlines the basic concept of the proposed method. That the system is stabilised without greatly changing the overall dynamics, i.e. the unstable period-1 becomes stable but does not change chape or location! To further justify this statement k_2 was kept

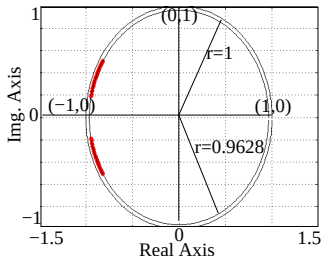

Fig. 8. The eigenvalues loci after positive current feedback with gain $k_2 = 0.1$. $V_{\text{in}} \in (29-32)V$.

constant, and the input voltage V_{in} was further increased. At $V_{\text{in}} \approx 41$V (see Fig.9) the system again undergoes a smooth period doubling. Now, if k_2 is increased to a value of 0.314, it is observed that system again becomes stable as shown in Fig.9b.

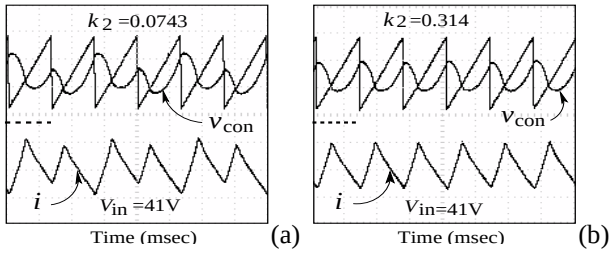

Fig. 9. Experimental observations showing the current feedback for enhancing the stability region: The control voltage and the inductor current for (a) the birth of period-2 orbit at V_{in}=41V, $k_2 = 0.0743$ and (a) stable period-1 orbit at $k_2 = 0.314$.

V. Conclusion

Using Filippov's approach, we have analysed the stability of periodic limit cycles of the voltage mode controlled buck converter. The method does not depend on the determination of the Poincaré map, and hence is quite suitable for stability analysis of the vast majority of power electronic systems whose Poincaré map cannot be determined in closed form. In this method the fundamental solution matrix over a complete cycle is determined by using the state transition matrices for the segments of the orbit lying in the individual matrix across the switching boundary. Based on the insight that this method offered we are able to propose various strategies to avoid fast scale instabilities. The methods that were rigorously analysed proposed a small change at the upper value of the saw-tooth signal and an addition of a value to the feedback control law that is proportional to the inductor current. Both methods changed the saltation matrix and hence forced the system to become stable without changing the shape and location of the orbit. Results have been analytically proven and experimentally validated.

Acknowledgments

The work was partially supported by the Department of Atomic Energy, Government of India under project no. 2003/37/11/BRNS

REFERENCES

[1] G. Yuan, S. Banerjee, E. Ott , and J. A. Yorke. Border-collision bifurcations in the buck converter. *IEEE Transactions on Circuits and Systems-I*, 45(7):707–716, July 1998.

[2] M. di Bernardo, F. Garofalo, L. Glielmo, and F. Vasca. Switchings, bifurcations and chaos in DC-DC converters. *IEEE Transactions on Circuits and Systems-I*, 45(2):133–141, 1998.

[3] A. El Aroudi and R. Leyva. Quasi-periodic route to chaos in a PWM voltage-controlled dc-dc boost converter. *IEEE Transactions on Circuits and Systems-I*, 48(8):967–978, August 2001.

[4] Z. T. Zhusubaliyev, E.A. Soukhoterin, and E. Mosekilde. Quasi-periodicity and border-collision bifurcations in a dc-dc converter with pulsewidth modulation. *IEEE Transactions on Circuits and Systems-I*, 50(8):1047–1057, August 2003.

[5] G. Poddar, K. Chakrabarty, and S. Banerjee. Experimental control of chaotic behavior of buck converter. *IEEE Transactions on Circuits and Systems-I*, 42(8):502–504, August 1995.

[6] T. Shinbrot, C. Grebogi, J. A. Yorke, and E. Ott. Using small perturbations to control chaos. *Nature*, (363):411–417, June 1993.

[7] P. So and E. Ott. Controlling chaos using time delay coordinates via stabilization of periodic orbits. *Physical Review E*, 51(4):2955–2962, 1995.

[8] K. Pyragas. Control of chaos via an unstable delayed feedback controller. *Physical Review Letters*, 86(11):2265–2268, March 2001.

[9] L. Fronzoni and M. Giocondo. Controlling chaos with parametric perturbations. *International Journal of Bifurcation and Chaos*, 8:1693–1698, 1998.

[10] R. Chacón and J. D. Bejarano. Routes to suppressing chaos by weak periodic perturbations. *Physical Review Letters*, 71:3103–3106, 1993.

[11] Y. Zhou, C. K. Tse, S. S. Qiu, and F. C. M. Lau. Applying resonant parametric perturbation to control chaos in the dc/dc converter with phase shift and frequency mismatch consideration. *International Journal of Bifurcation and Chaos*, 13(11):3459–3471, 2003.

[12] D. Giaouris, S. Banerjee, B. Zahawi, and V.Pickert. Stability analysis of the continuous conduction mode buck converter via Filippov's method. Under submission in IEEE Transactions on Circuits and Systems-I.